Accelerator Aspects of the Precision Mass Measurement Experiments at the VEPP-4M Collider with the KEDR Detector

S. A. Nikitin

for the VEPP-4 Team

BINP SB RAS

Introduction

Review of mass measurement experiments at VEPP-4

Mile stones

Particle	Energy, MeV	Relative accuracy	Detector	Years
J/ψ	3096.93 ± 0.10	3.2×10^{-5}	OLYa	1979–1980
$\psi(2s)$	3685.00 ± 0.12	3.3×10^{-5}	OLYa	1979–1980
Υ	$9460.57 \pm 0.09 \pm 0.05$	1.2×10^{-5}	MD-1	1983–1985
Υ'	10023.5 ± 0.5	5.0×10^{-5}	MD-1	1983–1985
Υ''	10355.2 ± 0.5	4.8×10^{-5}	MD-1	1983–1985
J/ψ	$3096.917 \pm 0.010 \pm 0.007$	3.5×10^{-6}	KEDR	2002–2005
$\psi(2s)$	$3686.119 \pm 0.006 \pm 0.010$	3.0×10^{-6}	KEDR	2002–2005
$\psi(3770)$	$3772.9 \pm 0.5 \pm 0.6$	2.1×10^{-4}	KEDR	2002–2005
D^0	$1865.43 \pm 0.60 \pm 0.38$	3.8×10^{-4}	KEDR	2002–2005
$D^\pm$	$1863.39 \pm 0.45 \pm 0.29$	2.9×10^{-4}	KEDR	2002–2005
τ	$1776.69^{+0.17}_{-0.19} \pm 0.15$	1.3×10^{-4}	KEDR	2005–2007

Top list of mass accuracy

Particle	$\Delta m/m$, *ppm*
n	0.04
p	0.04
e	0.04
μ	0.09
$\pi^\pm$	2.5
J/ψ	4.0
π^0	4.5
ψ'	5.0

O.V. Anchugov et al. Instruments and Experimental Techniques, 2010, Vol. 53, No. 1, pp. 15–2

What contributed

- Beam polarization measurement and beam energy monitoring methods developed and applied
- Problems on accuracy of energy calibration by spin precession frequency studied at new level
- Questions on optimal tuning of VEPP-4 systems and operation modes for obtaining and application of beam polarization in mass measurements set and solved

Methods for Beam Energy measurement

V.E. Blinov et al. NIMA 598 (2009) 23-30.

Resonant Depolarization technique

Spin precession frequency:

$$\Omega = \left(\frac{q_0}{\gamma} + q'\right) \cdot \langle B_\perp \rangle = \omega_0 \left(1 + \gamma \frac{q'}{q_0}\right) = \omega_0 (1+\nu)$$

$$\nu = \gamma \frac{q'}{q_0}$$

Spin tune-Energy relation:

$$E = \nu \cdot \frac{mc^2}{q'/q_0} = 440.64843(3)\ [\mathrm{MeV}] \cdot \nu$$

Limiting relative accuracy:

$$\delta E / E \sim 10^{-7}$$

External spin resonance:

$$\Omega \pm \omega_d = n \cdot \omega_0$$

- Energy error 2 keV (~10^{-6}), t ~ 1 sec
- Considerable sensitivity to beam and machine parameters
- No energy spread measurement
- Instant energy measurement

Compton Backscattering monitor

$$\omega_{max} = \frac{E^2}{(E + m_e^2/4\omega_0)} \simeq 4\gamma^2\omega_0$$

$$E = \frac{\omega_{max}}{2}\left(1 + \sqrt{1 + \frac{m^2}{\omega_0\omega_{max}}}\right)$$

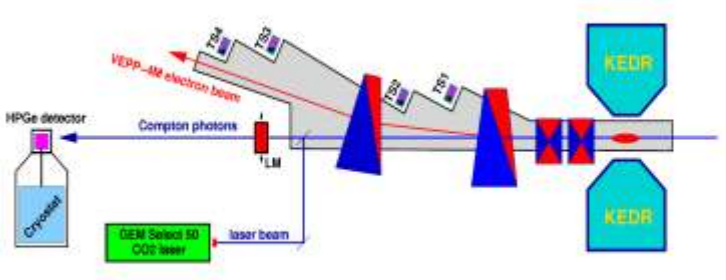

- Energy error 5 ⑨$10^{-5}$, t ~ 30 min
- Small sensitivity to beam and machine parameters ($\sigma_{laser} >> \sigma_{beam}$)
- Measure energy spread (10%)
- Energy monitoring

Absolute energy calibration by RD

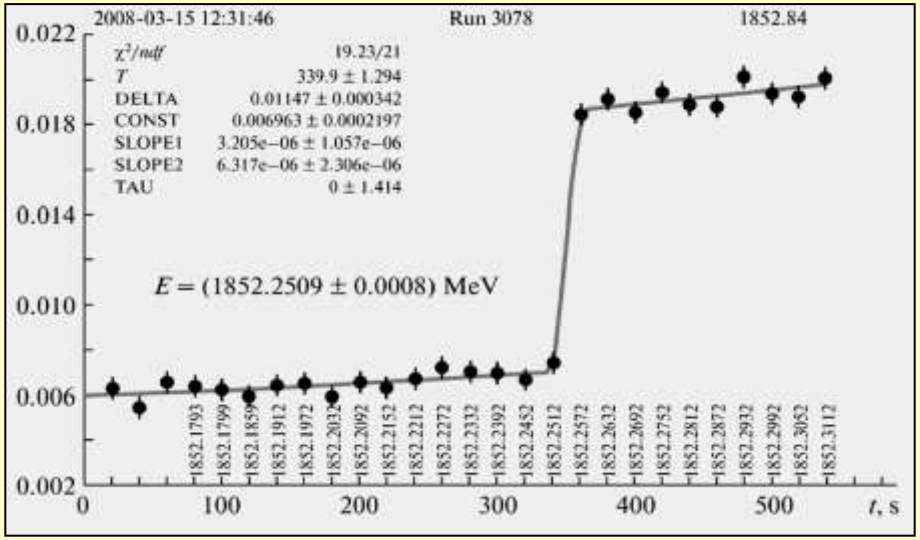

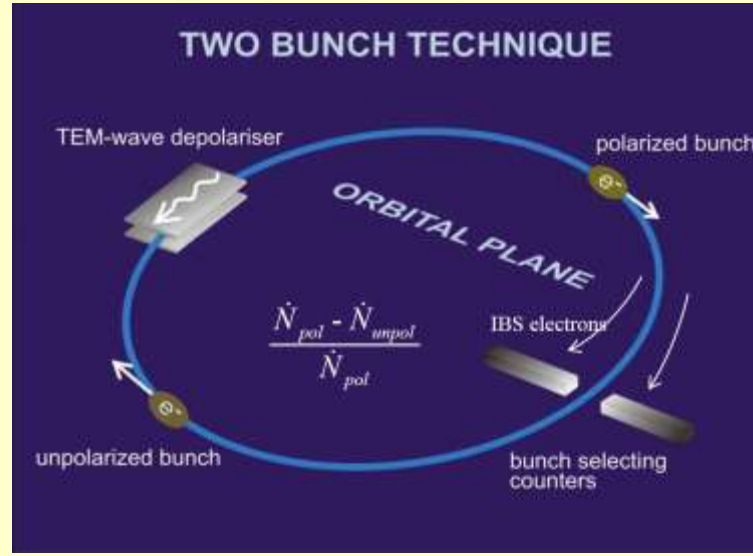

- Depolarization jump $\Delta\left(\frac{\dot{N}_{pol}-\dot{N}_{unpol}}{\dot{N}_{pol}}\right)\propto\zeta^2$
- Intra-Beam-Scattering rate up to ~ 1 MHz/mA
- Rb standard (10^{-10}) for both the RF and depolarizer systems
- Machine limit on accuracy:

  spin line width $\frac{\delta E}{E}=\frac{\delta\nu}{\nu}\sim\left\langle H''(\sigma_{x\beta}^2+\sigma_{x\gamma}^2)\right\rangle\sim 5\cdot 10^{-7}$
- Typical error: δE=2 keV (10^{-6})
- To date more 3000 RD calibrations

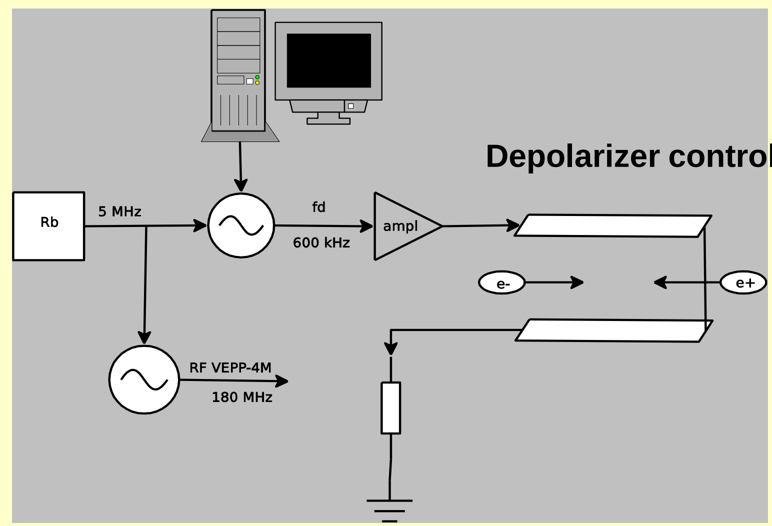

VEPP-4 layout with the polarization manipulation and measurement devices

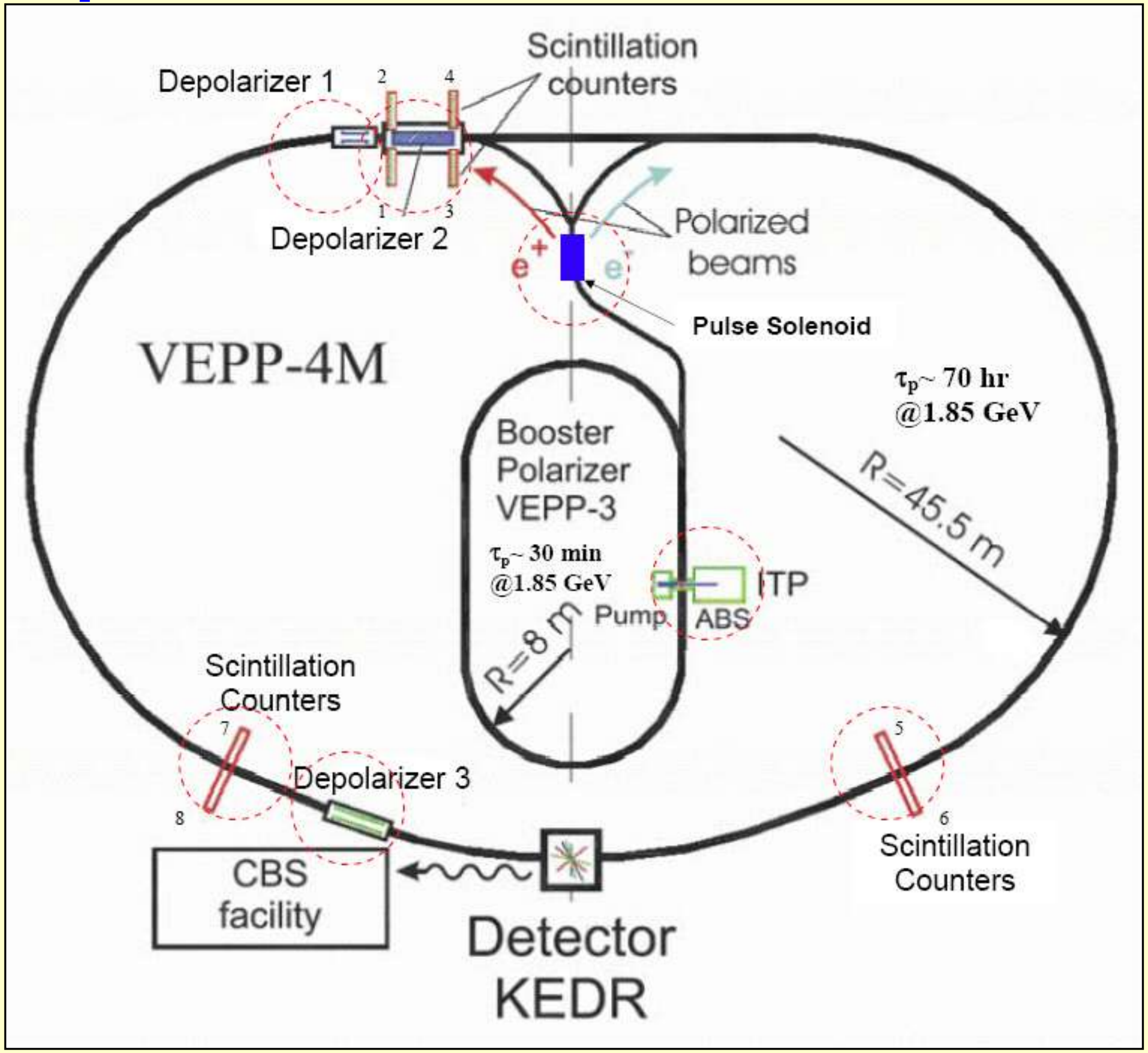

Obtaining of polarized beams

- Suitable radiative polarization time in the VEPP-3 booster

$$\tau_{pol}[hr] \approx \frac{12}{E^5[GeV]} \approx 33\,\mathrm{min}\ @\,1.85\,\mathrm{GeV}$$

- Too long desing radiative polarization time at VEPP-4M

$$\tau_{pol}[hr] \approx \frac{1540}{E^5[GeV]} \approx 70\,\mathrm{hr}\ @\,1.85\,\mathrm{GeV}$$

- 3D spin kinematics in the VEPP-3-VEPP-4M beam-line results in decrease of the e+ polarization degree in the domain of 1.85 GeV if no special measures are taken for spin manipulation
- Acceptable polarization life-time in VEPP-4M even at small off-tunings from the spin resonances
- VEPP-3 and VEPP-4M tunes ν_x, ν_y are kept in free cells of the spin resonant grid $\nu + m \cdot \nu_x + n \cdot \nu_y = k$ up to the $|m|+|n|=10$ order
- Feed back on the VEPP-3 work point stabilization $\delta(\nu_x, \nu_y) = \pm 0.002$

Beam polarization degree at VEPP-3

M.V. Dyug et al. NIMA 536 (2005) 338-343

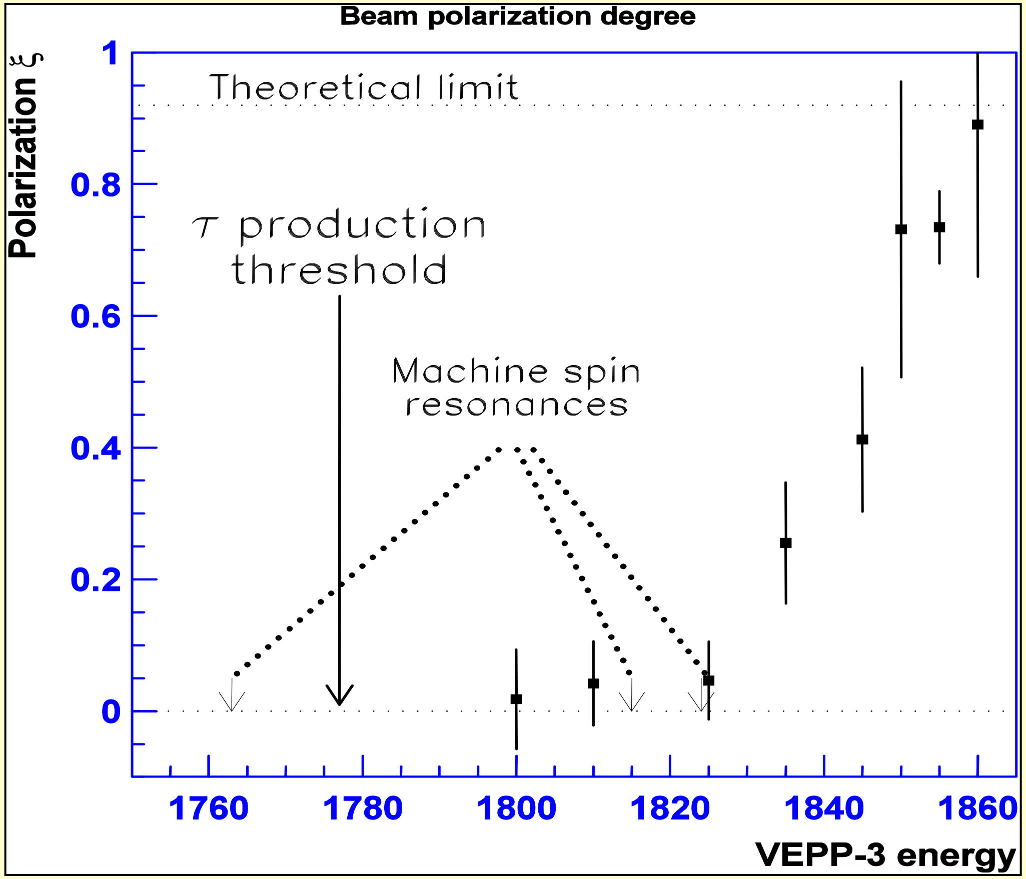

First Möller polarimeter
with Internal Polarized Target

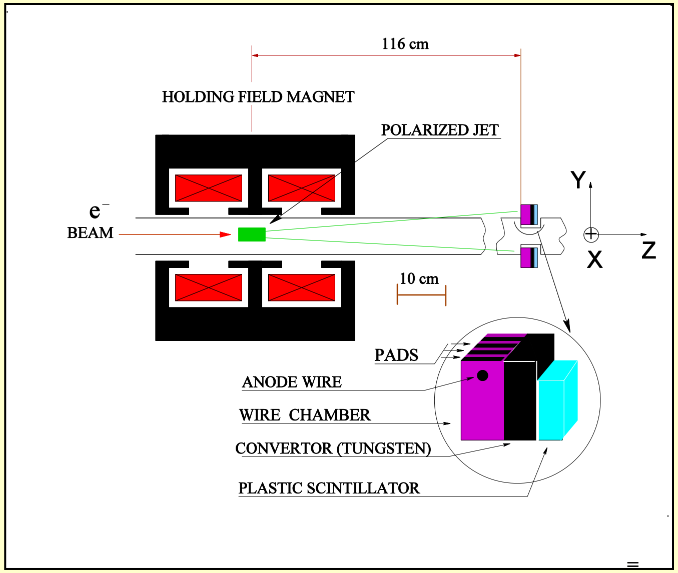

$$A = \frac{N_{\uparrow\uparrow} - N_{\uparrow\downarrow}}{N_{\uparrow\uparrow} + N_{\uparrow\downarrow}} = A_g \zeta_B \zeta_T, \quad A_g \approx 0.9$$

Deuterium Atomic Jet has the electron polarization Pe≈1.
Target thickness of 5×10^{11} electrons/cm^2
``Holding'' field of 300-400 gauss varied in a sign
Counting rate of 6 Hz at I=100 mA.

Solution of the polarized e+ beam injection problem

Vertical spin proection of injected polarized beams vs Energy

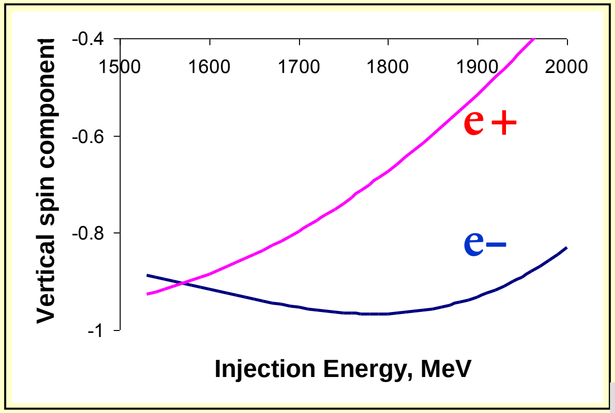

Pulse solenoid layout

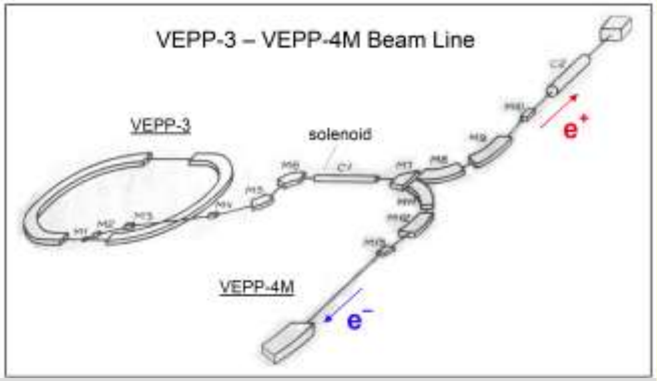

First proposal: O.N. Gordeev et al. Preprint 83-110. Realized in 2007: V. Blinov et al. Beam Dynamics NewsLetter, No. 48, 207-217

Vertical spin projection of positrons vs the solenoid strength

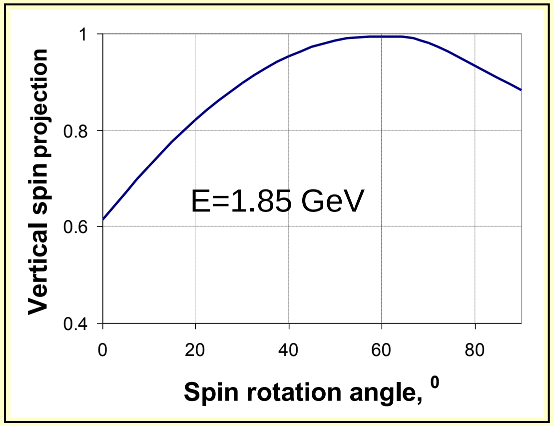

Solution: 2.5 Tesla·meter pulse solenoid in the VEPP-3-VEPP-4M beam-line

Experiment: 1.5 times vertical e+ spin projection increase,
2 times depolarization jump increase (2.5 times calc.)

Advantage: precise measurement of the energy gap between e+ and e- (~1 keV)

Analysis of Polarization Life-Time nearby the tau-lepton threshold energy

A.Bogomyagkov et al. EPAC'04 Proc. , pp. 737-739

Depolarization by quantum fluctuations (QF)

–vertical disalignment of focusing magnets

–vertical orbit bumps

–coupling due to lens and bend magnet rotations

–coupling due to vertical orbit distortion in sextupoles

–synchrotron modulation of spin frequency

–betatron oscillations in sextupoles

Resonance spin diffusion at ripples in the 25-30 KHz range (?)

PWM corrector power supply: f=(1, 2, 3)⑨12.5 kHZ, σ_v=1.4 kHz

VEPP-4M

E=1777 MeV

v – 4=0.03 <<1 (27 kHz)

T_{pol} =87 hr

T_r /T_{pol} << 1

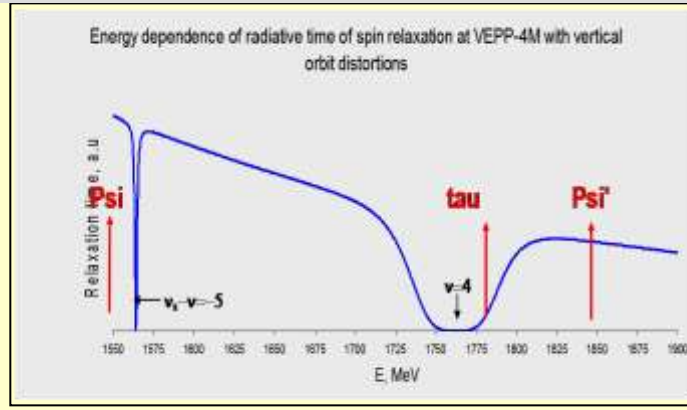

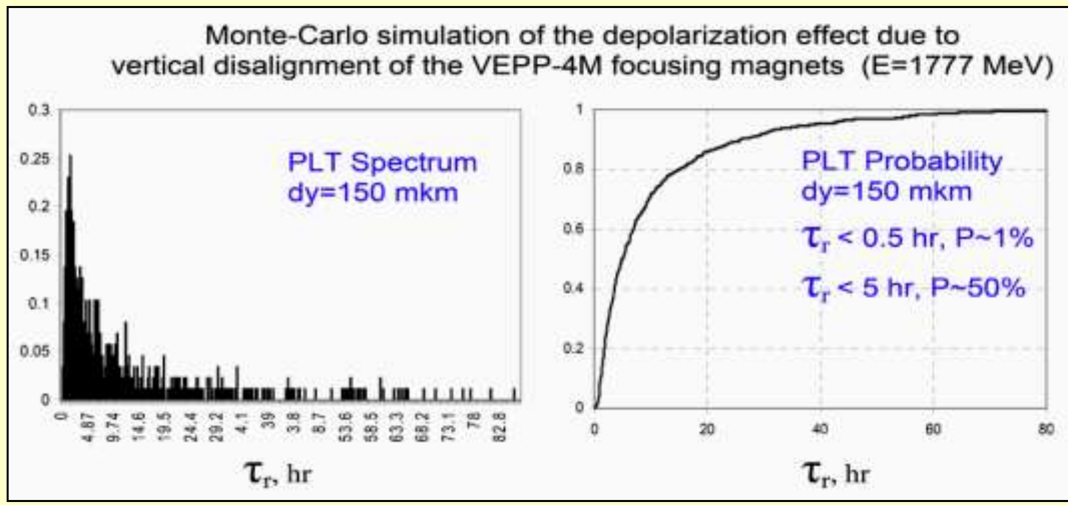

QF-based depolarization models: τ_r ≥1 hr most likely

Experimental data on polarization at the tau-threshold

Work Cycle

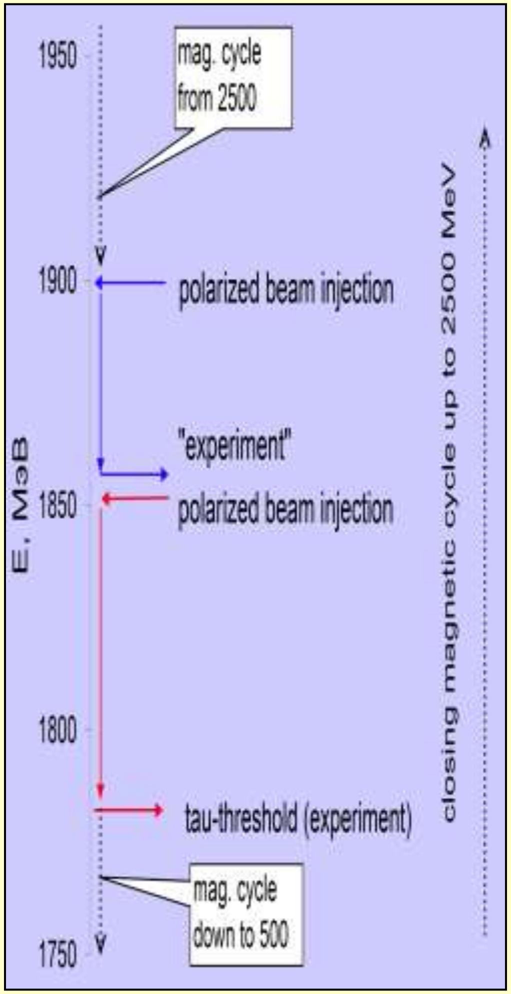

Tuning Stage

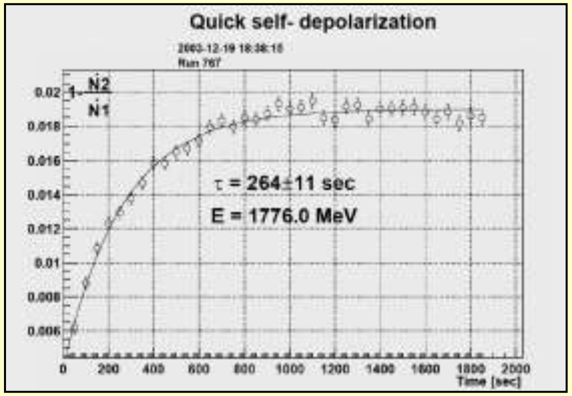

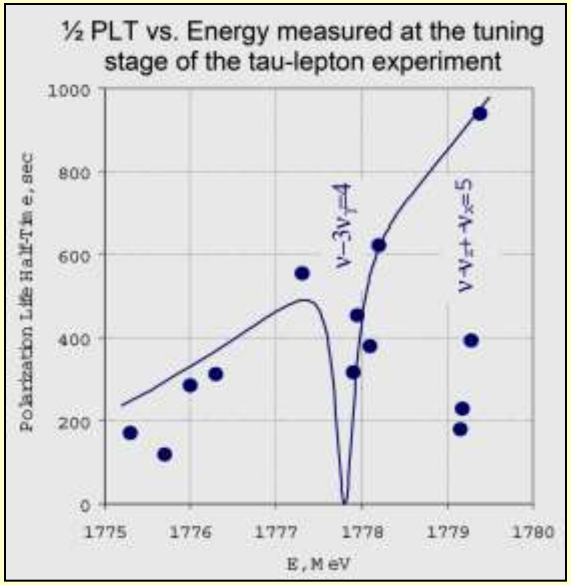

Regular Runs in 2005-2008

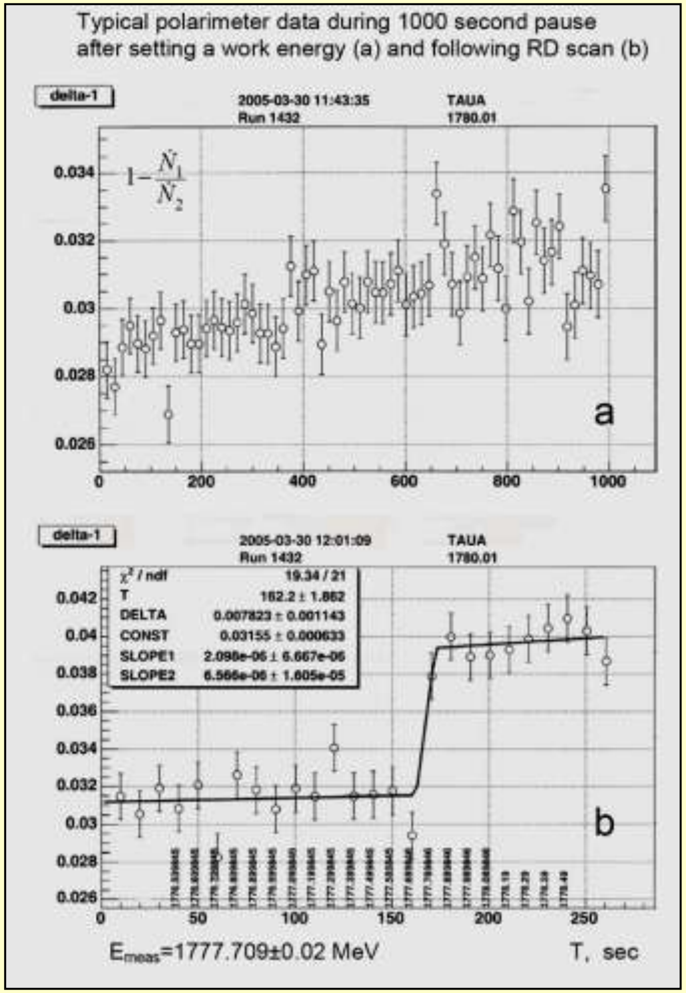

Questions on Accuracy

- Accuracy of instant absolute energy calibration
- Modulation spin resonances
- Spin tune shift not conserving the “spin tune - energy” ratio
- Effect of orbit corrections on energy
- Central mass energy determination
- Energy and energy spread stability

Field ripples as a hazard in RD technique

$$H = H_0 + \Delta H \cos \nu_H \theta \;\rightarrow\; \nu = \bar{\nu} + \Delta \cdot \cos \nu_H \theta \;\rightarrow\; \nu = \bar{\nu} + l \cdot \nu_H \pm \nu_d = k$$

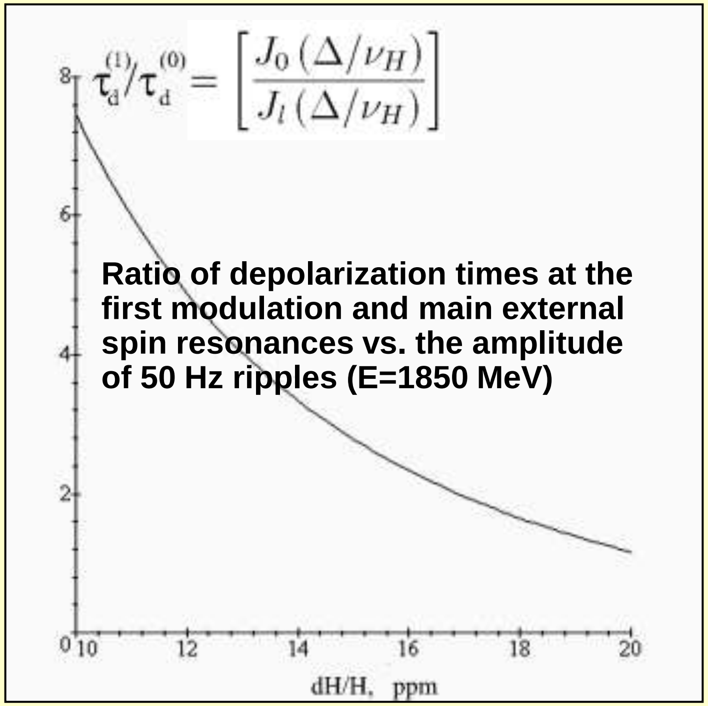

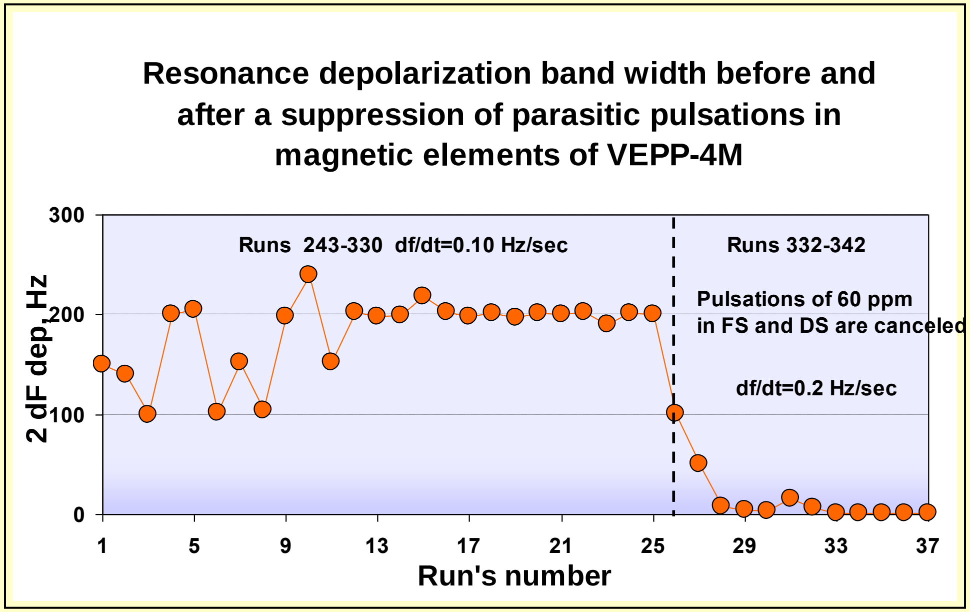

Energy error: 10^{-4} $\longrightarrow$ 10^{-6}

Depolarizer operation mode tuning:

- Depolarizing efficiency batching at a level sufficient just for the main spin resonance (most powerful) and not affecting modulation ones
- Crucially depends on correctness of the Spin Response Function (F^{ν}) calculation

Spin Response Function

Ya.S. Derbenev, A.M. Kondratenko, A.N. Skrinsky. Part.Acc., 1979, V.9, N4

$$F^{\nu}(\theta) = \frac{\nu}{2} e^{i\nu\theta} \left[f_z \int_{-\infty}^{\theta} \overline{f'_z} \mathcal{K} e^{-i\nu\phi} d\theta' - \overline{f_z} \int_{-\infty}^{\theta} f'_z \mathcal{K} e^{-i\nu\phi} d\theta' \right]$$

Design characteristic like β-function
Energy and azimuth dependent
Resonance at $\nu \pm \nu_z = m \cdot l$
m, the super-period number

Transverse field depolarizer efficiency
$\tau_d^{-1} \propto |F^{\nu}|^2$
Local value variation ~1÷100

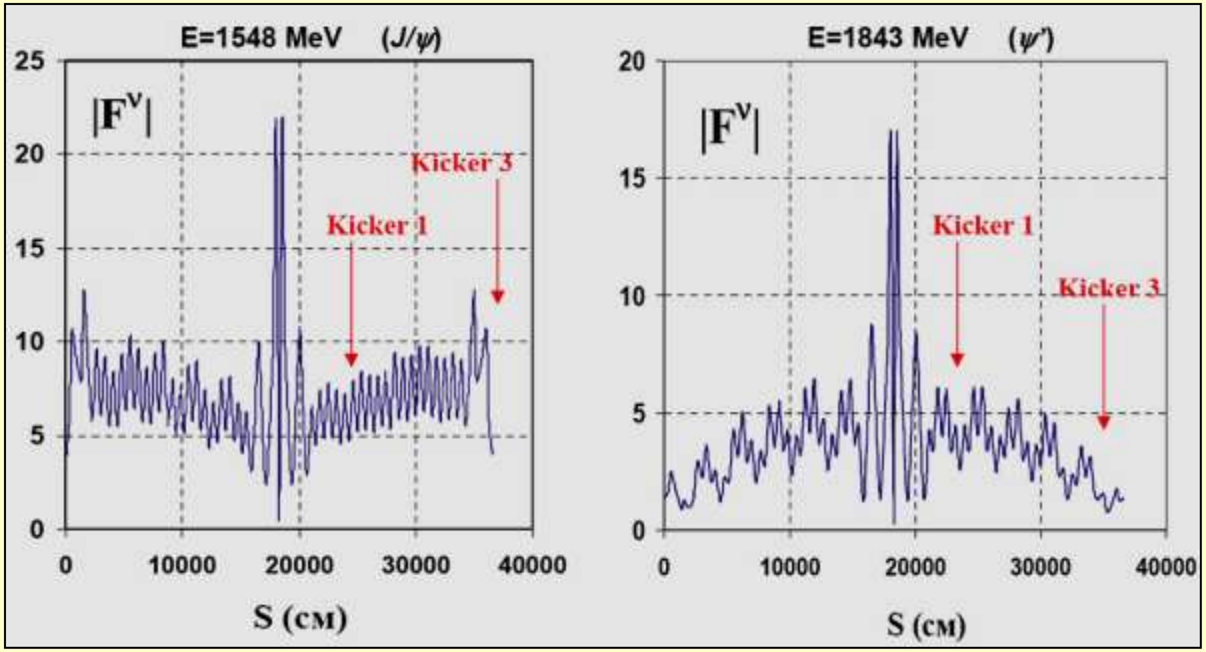

- We choose Kicker 1 or Kicker 3 as the depolarizer depending on the work energy domain
- We properly tune the depolarizer scan mode (scan rate and voltage at plates)

S.Nikitin. Preprint ИЯФ 2005-54

Spin tune shift due to vertical closed orbit distortions

A.V. Bogomyagkov, S.A. Nikitin, A.G. Shamov. RUPAC 2006 Proceedings.

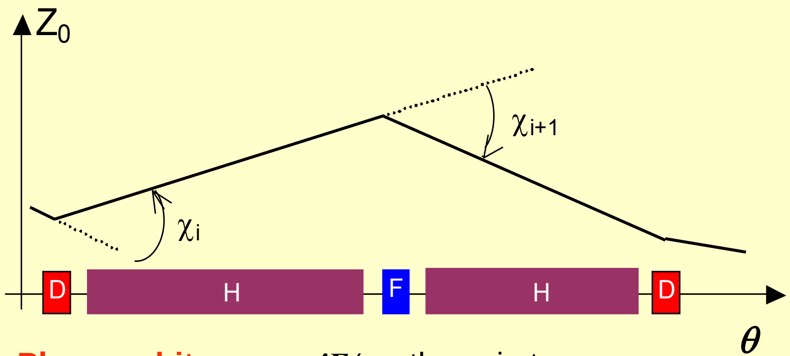

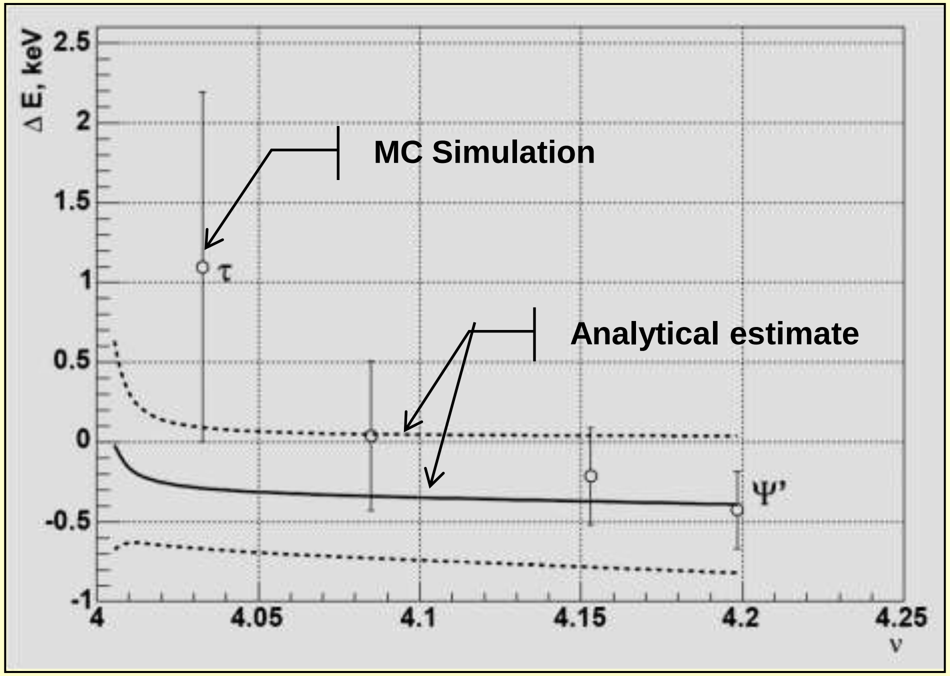

Planar orbit $\rightarrow \nu = q'E/ec$, the spin tune

$2\cos\pi\nu = Tr\ \Lambda$

Λ= 2×2 matrix of spin rotation about the vertical axis

Non-planar orbit $\rightarrow \nu \approx q'E/ec + \Delta\nu\,(E, perturbations)$

$\Lambda' = \Lambda + \Delta\Lambda = \prod \Lambda_i$, a matrix product of spin rotations about arbitrary axes

$\Delta\nu \approx -Tr\,(\Delta\Lambda)/(2\pi\sin\pi\nu)$

$$\Delta\nu \approx \frac{\nu^2}{8\pi\sin\pi\nu}\left[\cos\pi\nu\sum_i \chi_i^2 + \sum_{\substack{i,j\\ i\neq j}} \chi_i\chi_j\cos(\pi\nu - |\Phi_{ij}|)\right],\quad \Phi_{ij} = \nu\int_{\theta_i}^{\theta_j}\frac{H}{\overline{H}}d\theta$$

$$E = 1777\ \text{MeV},\ \left\langle Z_0^2\right\rangle^{1/2} \approx 1.2\ \text{mm}\ \rightarrow\ \frac{\Delta\nu}{\nu} \sim 10^{-6},\ \Delta E = 1.5 \pm 1.5\ \text{keV}$$

Spin tune shift due to KEDR field compensation error

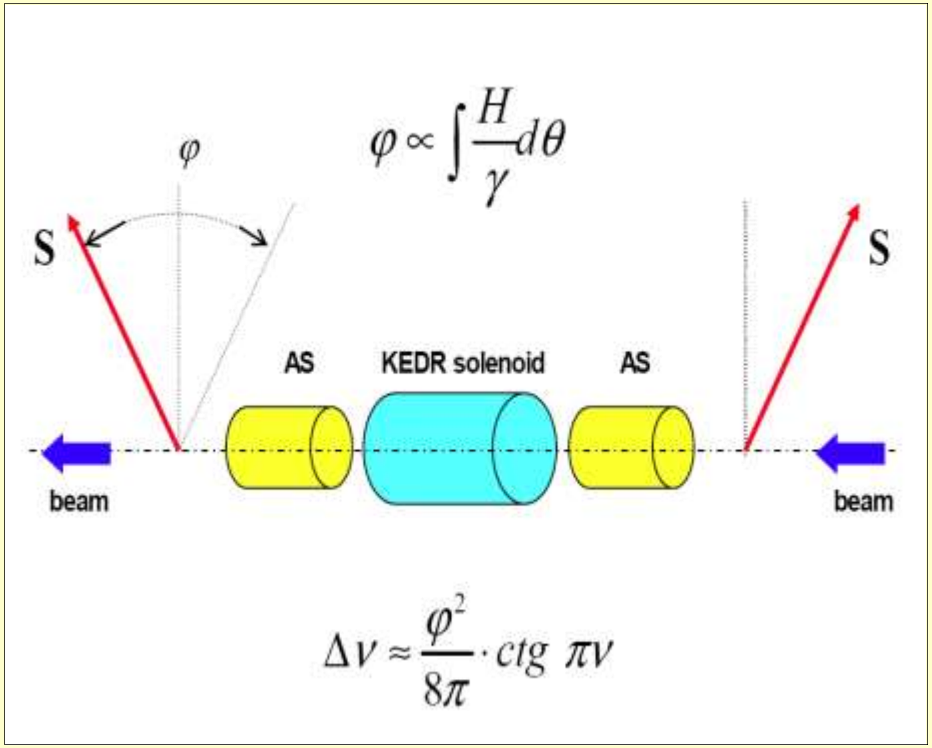

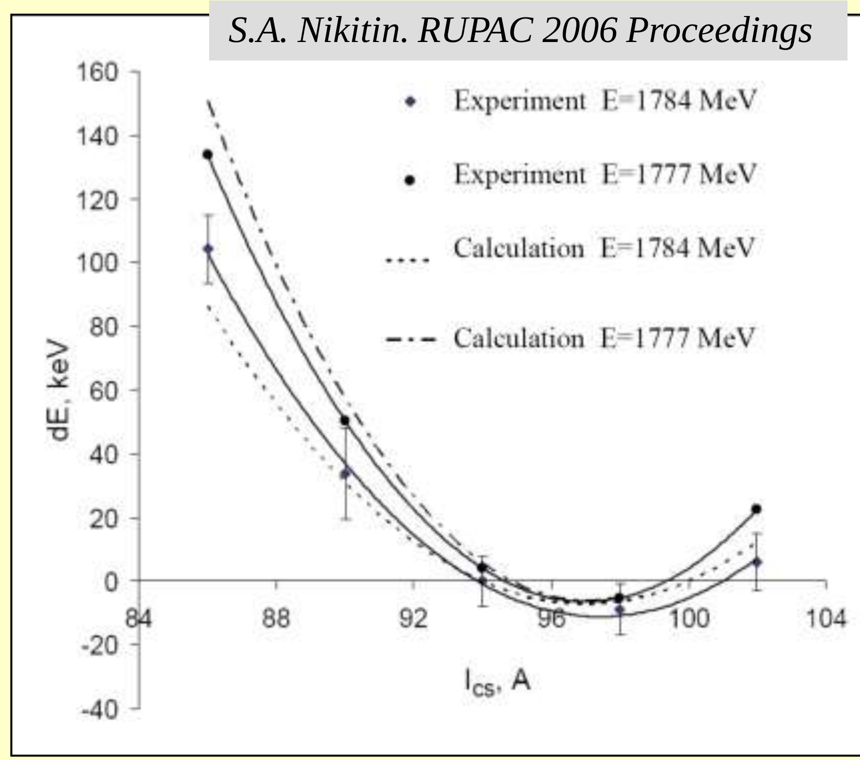

Advantages:

- Optimal compensation solenoid coil current I_{cs}(opt)=97 A
- Optimal ratio to the detector field I_{cs}(opt)/H_{KEDR} =16.13 A/kgs
- Systematic energy error reduction down to ~1 keV
- Betatron coupling minimization due to RD technique with an accuracy ~1% in adjusting I_{cs}

Energy shift due to radial orbit correctors

V.E. Blinov et al. NIMA 494 (2002) 81-85

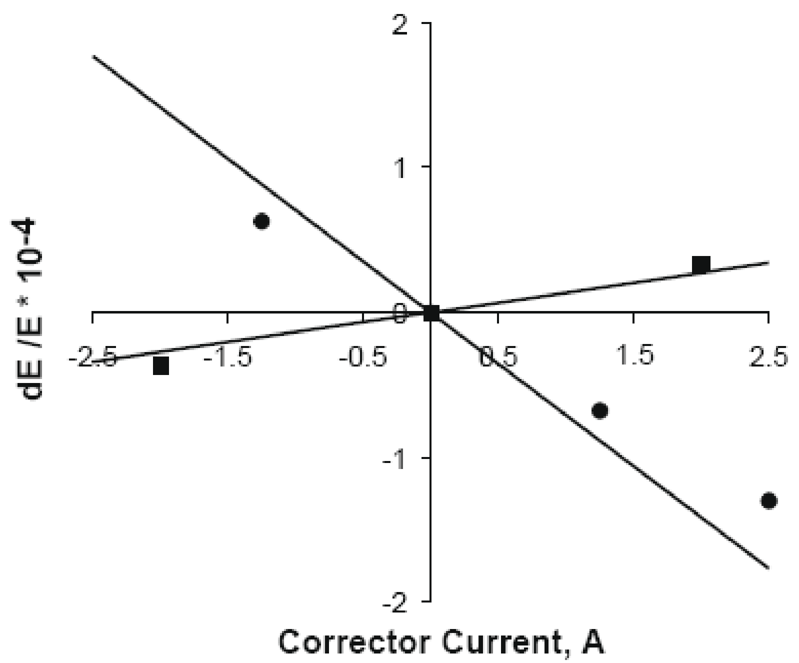

Fig. 3. Energy effect of one of the X-correctors in arcs ($\eta_X = 80$ cm, the deflection efficiency $C = 0.55$ mrad/A—the circles) and one in the straight section ($\eta_X = -31$ cm, $C = 0.28$ mrad/A—the squares).

$$\frac{\Delta E}{E} = -\frac{\eta_x}{\alpha \Pi} \cdot \theta$$

θ – radial deflection angle
η_x – dispersion function
α – momentum comp. factor
Π – machine perimeter

Relation between the relative energy shift ε and the RMS orbit distortion δx

$$\frac{\varepsilon}{\delta x} \sim \frac{2\sqrt{2}\sin(\pi \nu_x)}{\alpha L} \frac{\bar{\eta}_x}{\bar{\beta}_x}$$

$\varepsilon \sim 5\times10^{-6}$ at $\delta x \sim 100$ mkm

Orbit and corrector monitoring during luminosity run between RD calibrations

Effect of vertical bumps on energy and spin tune shift

Magnet/Electrostatics Bumps in the Technical straight section with the parasitic I.P. (**C**):

$$\frac{\Delta E}{E} = -\frac{1}{2\alpha\Pi} \cdot \int y_0'^2 ds,$$

the "lengthening orbit" effect , the same for e+/e-.

Electrostatics Bumps at the arc sections with parasitic interaction points (**B**):

- ΔE/E due to the "lengthening orbit" effect
- system. error due to the spin tune shift

(precession in a sequence of H_x- and H_y- fields)

"Magnet" Bump over the experimental section with the main I.P. (**A**):

- ΔE/E due to the "lengthening orbit" effect
- system. error due to the spin tune shift

(because of intermediate bend magnets)

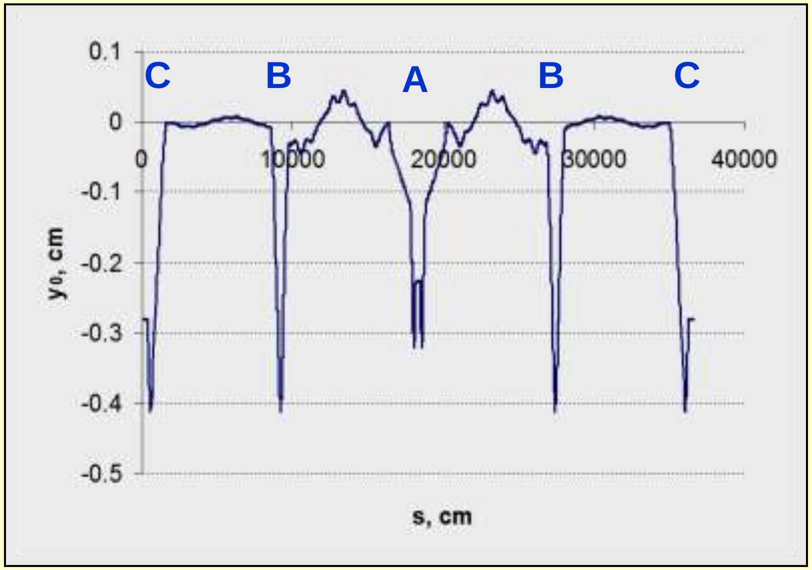

Table 1: Invariant mass correction, $E = 1850$ MeV.

Origin place	amplitude of the separation, mm	$2\Delta E$, keV
arcs	4	-4
technical area	5	-4.6

Energy loss distribution and C.M. energy determination by RD data

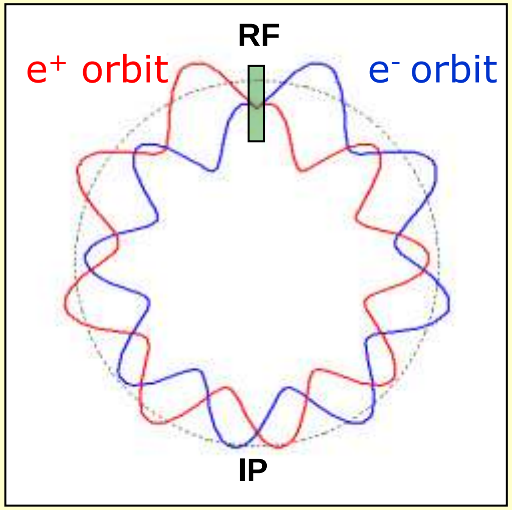

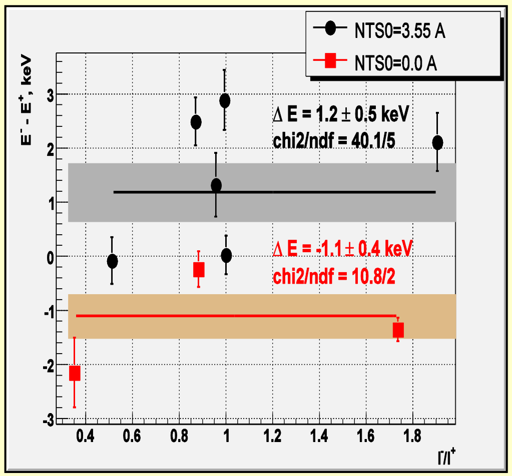

Energy difference of e+ and e- in simultaneous measurements

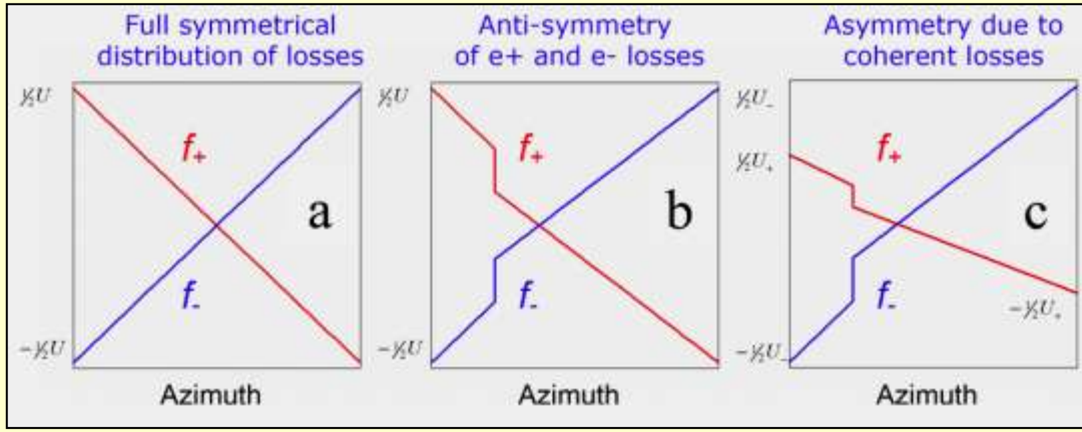

$$E_{\pm}(\theta) \to E_0\left[1 + f_{\pm}(\theta) + \varepsilon\right]$$

a) **Azim. Symm.:** $K = const,\ \eta_x = const$ **or Mirror Symm.:** $\langle f \rangle = \dfrac{\langle K\eta_x f\rangle}{\langle K\eta_x\rangle}$

$$\langle E\rangle = <E_-> = <E_+> = E_{RD} = E_0,$$

$$E_-(\theta) + E_+(\theta) = 2E_0 \equiv W, \quad \text{an invariant mass}$$

$$E_-(\theta) - E_+(\theta) = <E_-> - <E_+> \equiv 0$$

b) **Loss Function Anti-Symm. (wiggler magnets etc.):** $f_- = -f_+$

$$\delta = \frac{E_-(\theta) - E_+(\theta)}{E_0} = 2\frac{\langle K\eta_x\rangle \cdot f_- - \langle K\eta_x f_-\rangle}{\langle K\eta_x\rangle},$$

$$E_-(\theta) + E_+(\theta) = \langle E_-\rangle + \langle E_+\rangle = 2E_0 = W\left[1 + O(\delta^2)\right] \approx W$$

System. error in the C.M. energy: $\lambda = \dfrac{\langle E_-\rangle - E_0}{E_0} = \dfrac{1}{2}\cdot\dfrac{\langle E_-\rangle - \langle E_+\rangle}{\langle E_-\rangle}$ $\quad\lambda \sim 10^{-6}$

c) **Asymmetry from Coherent Losses at different e+/e- currents:** $f_- \neq -f_+$

$$E_-(\theta) + E_+(\theta) = E_0 \cdot \left(2 + f_- + f_+ - \frac{\langle K\eta_x f_-\rangle + \langle K\eta_x f_+\rangle}{\langle K\eta_x\rangle}\right)$$

Some corrections to C.M. energy determination

Asymmetry of Luminosity distribution in energy

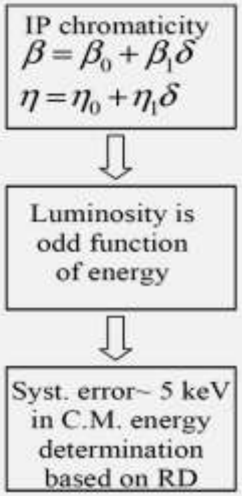

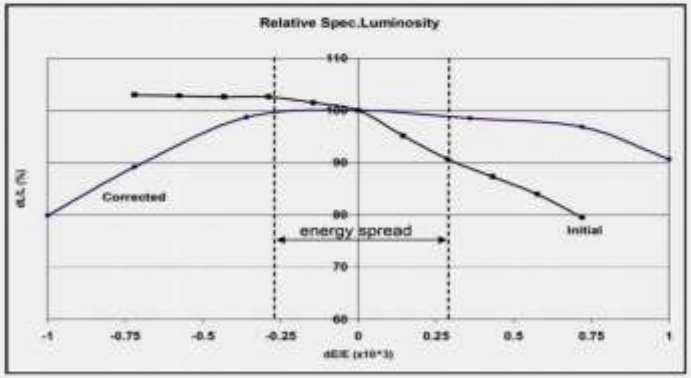

Specific luminosity vs. revolution frequency before and after IP chromaticity correction

A.Bogomyagkov et al., PAC 2007 Proceedings, MOOBI01, p.63

Effect of beam potential

V.I. Telnov (2003)

Beam Potential: $e\Phi = e\lambda(z)\left(C + \ln 2 - 2\ln\left(\frac{\sigma_x(s)+\sigma_y(s)}{r(s)}\right)\right)$

Average energy: $E = E_{mech,ring} + e\Phi_{ring}/2 = E_{mech,IP} + e\Phi_{IP}/2$

Mass of particle produced in e+e- annihilation:

$$Mc^2 = 2E_{mech,ring} + e\Phi_{ring} + e\Phi_{IP}$$

Energy measured by RD: $E_{meas} = E_{mech,ring}$

Mass correction: $\Delta M = e\Phi_{ring} + e\Phi_{IP} \sim 1.8$ keV (VEPP-4M)

A.Bogomyagkov, S. Nikitin, V.Telnov, G.Tumaikin. APAC 2004 Proc., TUP-11002.

Other sources of error

- Beam angular and energy spread (invariant mass correction ~ 0.3 keV)
- Beam separation in parasitic IPs (invariant mass correction ~ 5 keV)
- Vertical dispersion of opposite sign for e+ and e- in conjunction with non-zero separation in IP (due to beam-beam effect or perturbations from beam separation in parasitic IPs)

Beam energy spread

Physicists demand:
in narrow resonance measurements (ψ–family) $\delta\sigma_E$ < a few %
at tau-lepton threshold $\delta\sigma_E \sim$ 5-10 %

Energy spread measurement *O.I. Meshkov et al., J. Inst. 2 N 6 (June 2007)*

1. Fit of the measured betatron oscillation envelope

$$A(t) \propto \exp\left(-\frac{t^2}{2\tau^2}\right) \cdot \exp\left(-\left(\frac{\partial\omega_\beta}{\partial E}\frac{\sigma_E}{\omega_s}\right)^2 \cdot (1-\cos(\omega_s t))\right), \quad \tau^{-1} = 2\frac{\partial\omega_\beta}{\partial a^2} b \cdot \sigma_y$$

N.Vinokurov, G.Kulipanov, V.Korchuganov, E.Perevedentsev. Preprint ÈßÔ 76 – 87.

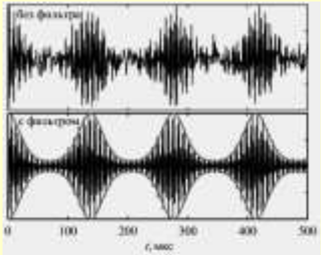

2. Measurement of amplitude ratio of synchrotron satellites to the main betatron peak in dependence of chromaticity

$$R_m(y) = \frac{1}{y^2}\int_0^\infty J_m^2(x) e^{-\frac{x^2}{2y^2}} x\,dx, \quad y = \left(\frac{\omega_\beta \alpha}{\omega_s} + \frac{\omega_0 C_y}{\omega_s}\right)\sigma_E$$

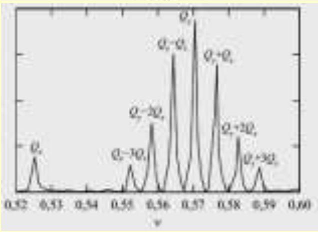

3. Fit of the edge of Compton back-scattering spectrum

$$E = \frac{\hbar\omega_m}{2}\left(1 + \sqrt{1 + \frac{m_e^2 c^4}{\hbar^2 \omega_m \omega_0 \sin^2\frac{\alpha}{2}}}\right)$$

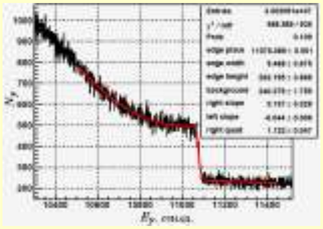

Energy spread control

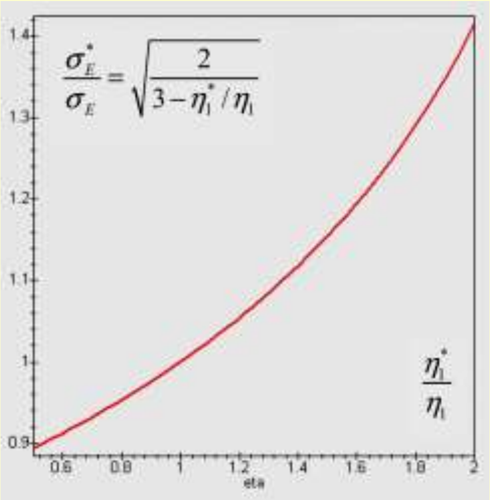

Change in energy spread vs relative disturbance of dispersion in the dipole-gradient wigglers

Energy stability

O.V. Anchugov et al. Instrumental and Experimental Techniques, 2010, Vol. 53, No. 1, pp. 15-28.

V.E.Blinov et al. Beam Dynamics Newsletter, 2009. No. 48, pp. 207-217.

Round-the-clock energy variations (no thermo-stabilization)

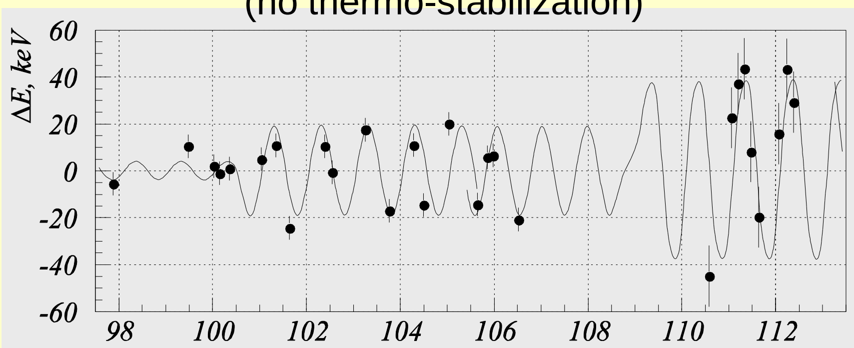

Thermal stabilization

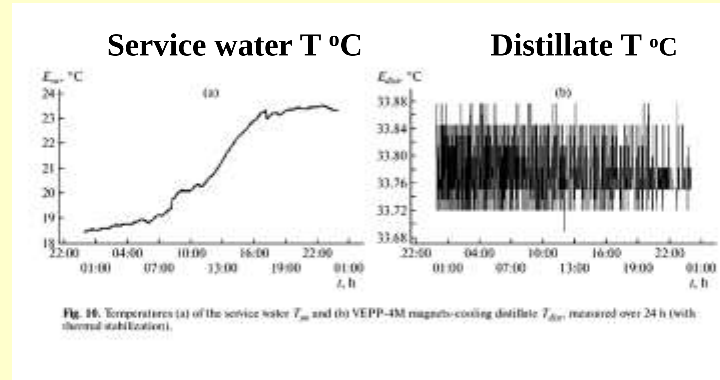

Long-term energy stability with thermo-stabilization

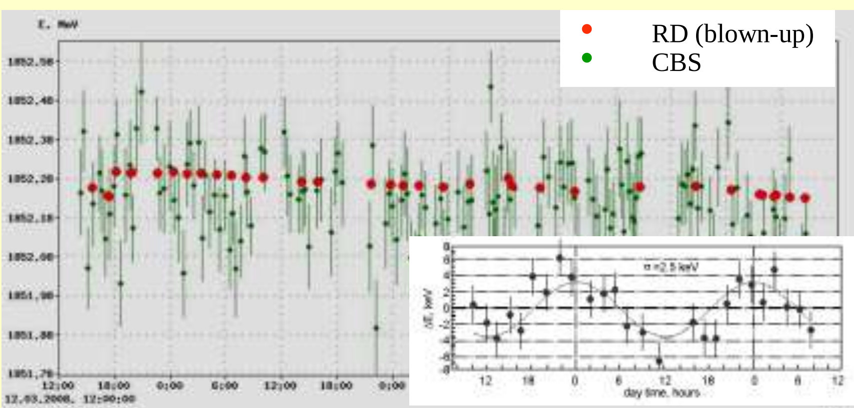

NMR data-based Feed Back Loop

NMR magnetometer monitoring data on the reference magnet field.

NMR data were read with a period of several seconds.
Feedback band ~ 0.1 Hz .
Long-term field stability ~10^{-6}.

Daily beam energy drift with the field feedback loop on ~ 1 keV

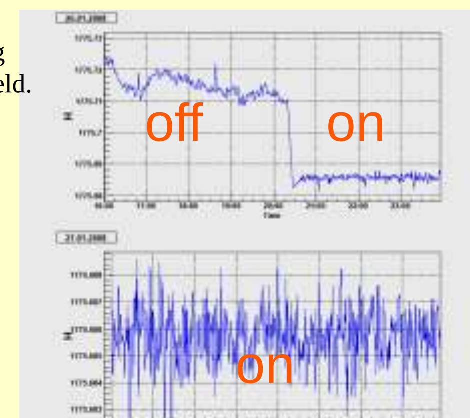

For the experiment with ~10^{-9} depolarization frequency resolution

Acknowledgements

Thanks to V.Smaluk, S.Karnaev and V.Kiselev for help in material preparation.

Thank you for attention!